

This discussion paper is/has been under review for the journal Biogeosciences (BG).  
Please refer to the corresponding final paper in BG if available.

# Rapid establishment of the CO<sub>2</sub> sink associated with Kerguelen's bloom observed during the KEOPS2/OISO20 cruise

C. Lo Monaco, N. MetzI, F. D'Ovidio, J. Llort, and C. Ridame

UPMC-CNRS-IRD-MNHN, LOCEAN Laboratory, 4 place Jussieu, 75005 Paris, France

Received: 20 November 2014 – Accepted: 24 November 2014 – Published:  
17 December 2014

Correspondence to: C. Lo Monaco (claire.lomonaco@locean-ipsl.upmc.fr)

Published by Copernicus Publications on behalf of the European Geosciences Union.

**BGD**

11, 17543–17578, 2014

## Rapid establishment of the CO<sub>2</sub> sink

C. Lo Monaco et al.

Title Page

Abstract

Introduction

Conclusions

References

Tables

Figures

◀

▶

◀

▶

Back

Close

Full Screen / Esc

Printer-friendly Version

Interactive Discussion



## Abstract

Iron and light are the main factors limiting the biological pump of CO<sub>2</sub> in the Southern Ocean. Iron fertilization experiments have demonstrated the potential for increased uptake of atmospheric CO<sub>2</sub>, but little is known about the evolution of fertilized environments. This paper presents observations collected in one of the largest phytoplankton bloom of the Southern Ocean sustained by iron originating from the Kerguelen Plateau. We first complement previous studies by investigating the mechanisms that control air–sea CO<sub>2</sub> fluxes over and downstream of the Kerguelen Plateau at the onset of the bloom based on measurements obtained in October–November 2011. These new observations show the rapid establishment of a strong CO<sub>2</sub> sink in waters fertilized with iron as soon as vertical mixing is reduced. The magnitude of the CO<sub>2</sub> sink was closely related to chlorophyll *a* and iron concentrations. Because iron concentration strongly depends on the distance from the iron source and the mode of delivery, we identified lateral advection as the main mechanism controlling air–sea CO<sub>2</sub> fluxes downstream the Kerguelen Plateau during the growing season. In the southern part of the bloom, situated over the Plateau (iron source), the CO<sub>2</sub> sink was stronger and spatially more homogeneous than in the plume offshore. However, we also witnessed a substantial reduction in the uptake of atmospheric CO<sub>2</sub> over the Plateau following a strong winds event. Next, we used all the data available in this region in order to draw the seasonal evolution of air–sea CO<sub>2</sub> fluxes. The CO<sub>2</sub> sink is rapidly reduced during the course of the growing season, which we attribute to iron and silicic acid depletion. South of the Polar Front, where nutrients depletion is delayed, we suggest that the amplitude and duration of the CO<sub>2</sub> sink is mainly controlled by vertical mixing. The impact of iron fertilization on air–sea CO<sub>2</sub> fluxes is revealed by comparing the uptake of CO<sub>2</sub> integrated over the productive season in the bloom, between 1 and 1.5 mol C m<sup>-2</sup> yr<sup>-1</sup>, and in the iron-poor HNLC waters, where we found a typical value of 0.4 mol C m<sup>-2</sup> yr<sup>-1</sup>. Extrapolating our results to the ice-free Southern Ocean (~ 50–60° S) suggests that iron fertilization of the whole area would increase the contemporary oceanic uptake of

## Rapid establishment of the CO<sub>2</sub> sink

C. Lo Monaco et al.

Title Page

Abstract

Introduction

Conclusions

References

Tables

Figures



Back

Close

Full Screen / Esc

Printer-friendly Version

Interactive Discussion



CO<sub>2</sub> by less than 0.1 Pg C yr<sup>-1</sup>, i.e., less than 1 % of the current anthropogenic CO<sub>2</sub> emissions.

## 1 Introduction

The Southern Ocean plays a major role in moderating global warming by absorbing annually around 1 Pg (10<sup>15</sup> g) of carbon (Takahashi et al., 2009; Lenton et al., 2013). Although this number amounts to about 10 % of the CO<sub>2</sub> currently released to the atmosphere by human activities (mostly fossil fuel burning and land use change; Le Quéré et al., 2014), it hides a much larger potential because of iron limitation (Martin et al., 1990). Indeed, most of the CO<sub>2</sub> uptake occurs in the frontal region between 40 and 50° S where iron is available to sustain primary production, whereas south of the Polar Front (~ 50° S) stands the largest High Nutrient Low Chlorophyll (HNLC) area (Tagliabue et al., 2012). Iron enrichment experiments conducted in the HNLC region have demonstrated the role of iron in controlling primary production and the potential for increased uptake of atmospheric CO<sub>2</sub> when photosynthesis is stimulated (Boyd et al., 2007). However, due to the limited area and the short time-scales involved in these studies, the long-term efficiency and the consequences of artificial iron fertilization are still very uncertain.

An alternative to assess the impact of iron fertilization on the uptake of atmospheric CO<sub>2</sub> is offered by naturally fertilized environments, notably over and downstream of the Kerguelen Plateau in the Southern Ocean, where a large phytoplankton bloom is observed every summer (e.g., Mongin et al., 2008). A previous study conducted in this region in February 2005 (KEOPS/OISO12 cruise) confirmed that natural iron fertilization enhances the biological uptake of CO<sub>2</sub> over the Plateau compared to the surrounding HNLC waters (Blain et al., 2007). These observations, however, were limited to the declining phase of the bloom in its southern part. Kerguelen's bloom covers hundreds of thousands km<sup>2</sup>, and since spatial heterogeneity can be anticipated, more observations were needed to accurately assess the impact of iron fertilization on air–sea CO<sub>2</sub> fluxes.

## Rapid establishment of the CO<sub>2</sub> sink

C. Lo Monaco et al.

Title Page

Abstract

Introduction

Conclusions

References

Tables

Figures

◀

▶

◀

▶

Back

Close

Full Screen / Esc

Printer-friendly Version

Interactive Discussion



**Rapid establishment  
of the CO<sub>2</sub> sink**

C. Lo Monaco et al.

[Title Page](#)[Abstract](#)[Introduction](#)[Conclusions](#)[References](#)[Tables](#)[Figures](#)[Back](#)[Close](#)[Full Screen / Esc](#)[Printer-friendly Version](#)[Interactive Discussion](#)

The KEOPS project was designed to achieve a better understanding of the mechanisms at play over and downstream of the Kerguelen Plateau, in order to assess the impact of iron fertilization on biogeochemical cycles and ecosystems. The KEOPS2 survey was conducted at the start of the productive season, in October–November 2011, and coupled with the 20th OISO cruise, with the objective of monitoring the establishment of the CO<sub>2</sub> sink associated with Kerguelen's bloom and investigating the mechanisms responsible for spatial and temporal variations in air–sea CO<sub>2</sub> fluxes in different regions of the bloom. In this paper, we first present underway measurements of CO<sub>2</sub> and related parameters collected during the KEOPS2/OISO20 cruise. This allows to evaluate and understand the evolution of air–sea CO<sub>2</sub> fluxes over the Plateau and in the plume offshore during the transition from winter conditions to the growing season. These new observations are discussed with regard to iron and other nutrients availability, lateral transport and vertical mixing. Next, we used all available observations from the Surface Ocean CO<sub>2</sub> Atlas (SOCAT, Bakker et al., 2014), merged with KEOPS and more recent OISO data, in order to evaluate the seasonal evolution of air–sea CO<sub>2</sub> fluxes in and out of Kerguelen's bloom, and thus quantify the impact of iron fertilization on the uptake of atmospheric CO<sub>2</sub>.

## 2 Material and methods

This work is primarily based on in situ measurements collected during the KEOPS2/OISO20 cruise. Sampling and measurement techniques are described below. In order to push our analysis further, we also evaluated the seasonal evolution of air–sea CO<sub>2</sub> fluxes using all the OISO/KEOPS data available to date (1998–2013), complemented by observations from four previous cruises (1991–1993) obtained from the SOCAT database (version 2.0; Bakker et al., 2014), as well as measurements obtained from the CARIOCA buoy launched during the KEOPS2 survey. Underway measurements of the fugacity of CO<sub>2</sub> (*f*CO<sub>2</sub>) obtained during all OISO cruises (including the two KEOPS surveys), are or will soon be available at the Carbon Dioxide Informa-

tion Analysis Center (CDIAC, <http://cdiac.ornl.gov/oceans>) and in the SOCAT database (<http://www.socat.info>). In addition to in situ measurements, we used satellite data to map chlorophyll *a* concentration (Fig. 1 produced with the Giovanni online data system, available at <http://disc.sci.gsfc.nasa.gov/>), and to compute climatological winds for air–sea CO<sub>2</sub> flux calculation (see Sect. 2.2).

## 2.1 Sampling strategy and measurement techniques

The study site is defined around the Kerguelen Plateau, from 64 to 75° E, and between 47 and 51° S (Figs. 1 and 2). This region includes various biogeochemical systems, from the typical High Nutrients Low Chlorophyll (HNLC) waters generally found south of the Polar Front (PF), to the highly productive waters over and downstream of the Plateau (Fig. 1). The most extensive survey dedicated to understanding the functioning of this iron fertilized environment was conducted during the KEOPS2/OISO20 cruise, when physicists, biogeochemists and biologists were brought together to investigate the mechanisms at play in different regions of the bloom. The previous KEOPS/OISO12 cruise, conducted in January–February 2005, involved as much expertise, but it was limited to the southern part of the bloom situated over the Plateau. Below we describe the sampling and measurement techniques followed during the KEOPS2/OISO20 cruise, which are very similar to those followed during the first KEOPS survey (Jouandet et al., 2008), and during all OISO cruises (Metzl et al., 1999; Jabaud-Jan et al., 2004; Metzl, 2009; Lourantou and Metzl, 2011).

The KEOPS2 survey was conducted onboard R.R.V. *Marion Dufresne* in 2011, from the 17 October, when the ship approached the Kerguelen Plateau on its western side, to the 21 November, when the ship headed north of Kerguelen Island (see cruise track in Figs. 1 and 2). Our work is mostly based on hydrological and biogeochemical properties measured underway in surface waters (~ 5 m depth). Underway surface measurements include the fugacity of CO<sub>2</sub> (*f*CO<sub>2</sub>), sea surface temperature (SST), sea surface salinity (SSS) and fluorescence. In addition, atmospheric CO<sub>2</sub> was measured

BGD

11, 17543–17578, 2014

## Rapid establishment of the CO<sub>2</sub> sink

C. Lo Monaco et al.

Title Page

Abstract

Introduction

Conclusions

References

Tables

Figures

◀

▶

◀

▶

Back

Close

Full Screen / Esc

Printer-friendly Version

Interactive Discussion



## Rapid establishment of the CO<sub>2</sub> sink

C. Lo Monaco et al.

Title Page

Abstract

Introduction

Conclusions

References

Tables

Figures

◀

▶

◀

▶

Back

Close

Full Screen / Esc

Printer-friendly Version

Interactive Discussion



every 4 h, and surface water samples were collected every 4 h for total CO<sub>2</sub> (*T*CO<sub>2</sub>), total alkalinity (TA), chlorophyll *a* and nutrients concentrations and every 8 h for salinity.

The technique for *f*CO<sub>2</sub> measurements was described in details by Poisson et al. (1993), Metzl et al. (1995, 1999) and Jabaud-Jan et al. (2004). In short, sea surface water is continuously equilibrated using a “thin film” type equilibrator thermostated with surface seawater. The CO<sub>2</sub> in the dried gas is measured with a non-dispersive infrared analyser (Siemens). The analysis of standard gases used for calibration indicated an accuracy to ±0.7 μatm. All *f*CO<sub>2</sub> values presented here are normalized to 1013 hPa. *T*CO<sub>2</sub> and TA were measured onboard, using a potentiometric method with a closed cell, and Certified Referenced Materials (CRMs, batch 111, provided by A. Dickson, SIO, University of California). Accuracy estimated from the CRMs analysis was ±4 μmol kg<sup>-1</sup> for both TA and *T*CO<sub>2</sub>. SST and SSS were obtained from two Sea-Bird thermosalinographs. SSS was checked against measurements performed onboard using a salinometer (Park et al., 2014). Accuracy for SSS was evaluated to ±0.005. Nutrients were also measured directly onboard using a Skalar auto-analyzer (Blain et al., 2014). Accuracy was determined by measuring certified standards (CERTIPUR, Merck): it was 3.5 % for nitrate and 2.2 % for silicic acid (Si(OH)<sub>4</sub>) for concentrations around 35 μmol kg<sup>-1</sup>. Underway chlorophyll *a* measurements were obtained by filtering between 1 and 2 L of seawater on 25 mm GF/F Whatman filters (pressure < 200 mbar). Filters were stored at -80 °C until measurements were performed at LOCEAN using a Hitachi F-4500 spectrofluorometer, after extraction of the filters in 90 % acetone, following the method described by Neveux and Lantoiné (1993). The precision of chlorophyll *a* measurements is typically around 5 %. We used chlorophyll *a* measurements to calibrate underway fluorescence data, but due to the poor correlation obtained (*r*<sup>2</sup> = 0.5), calibrated fluorescence data must be considered with care.

Water samples were also collected at depth using a rosette equipped with 22 Niskin bottles and a Seabird CTD (Conductivity-Temperature-Depth) sensors. We used the data obtained between 0 and 20 m to complement underway measurements, with the

## Rapid establishment of the CO<sub>2</sub> sink

C. Lo Monaco et al.

Title Page

Abstract

Introduction

Conclusions

References

Tables

Figures

◀

▶

◀

▶

Back

Close

Full Screen / Esc

Printer-friendly Version

Interactive Discussion



exception of chlorophyll *a* data as it was not obtained using the same technique (high performance liquid chromatography) as for underway surface data. CTD (Conductivity-Temperature-Depth) profiles were also obtained at all stations, allowing to evaluate the mixed layer depth. Most of the stations are situated along the north–south and east–west transects (along  $\sim 72^\circ$  E and  $\sim 48.5^\circ$  S), that cover the southern and eastern sides of the Plateau and the plume offshore (Fig. 1). Here we present measurements collected at the station A3 situated over the Plateau in the core of the southern bloom investigated during the first KEOPS survey, and which was revisited twice during the KEOPS2 survey and again during the following OISO cruises.

### 2.1.1 Air–sea CO<sub>2</sub> flux calculation

The net flux of CO<sub>2</sub> across the air–sea interface (FCO<sub>2</sub>) was calculated according to the following equation:

$$FCO_2 = k \cdot s \cdot \Delta fCO_2 \quad (1)$$

*k* is the piston velocity evaluated as a function of wind speed (Wanninkhof, 1992), *s* is the solubility of CO<sub>2</sub> in seawater calculated from in situ temperature and salinity after Weiss (1974), and  $\Delta fCO_2$  is the difference between the fugacity of CO<sub>2</sub> in surface waters and in the marine air above ( $\Delta fCO_2 = fCO_2 \text{ sea} - fCO_2 \text{ air}$ ). Positive values of  $\Delta fCO_2$  indicate an outgassing of CO<sub>2</sub> to the atmosphere (CO<sub>2</sub> source), and negative values indicate an uptake of CO<sub>2</sub> by the ocean (CO<sub>2</sub> sink). We used the mean *f*CO<sub>2</sub> air value of 388  $\mu\text{atm}$  based on measurements obtained at  $\sim 15$  m above the sea surface during the KEOPS2 survey, and the mean temperature and salinity values of 3 °C and 33.8, respectively. The mean CO<sub>2</sub> molar fraction *x*CO<sub>2</sub> measured onboard was  $391.3 \pm 0.6$  ppm during the survey around Kerguelen, and  $389.5 \pm 2$  ppm between 25 and 50 °S. The latter compares well with the mean *x*CO<sub>2</sub> of  $389.0 \pm 0.6$  ppm measured in October/November 2011 at the nearest atmospheric monitoring station situated on Amsterdam Island at 77.5° E, 38.3° S (M. Ramonet, personal communication, 2014).

We evaluated  $f\text{CO}_2$  using either wind speed measurements made onboard or climatological monthly winds computed from QuikScat satellite data (Level 3 surface wind speed obtained from the Physical Oceanography Distributed Active Archive Center at the NASA Jet Propulsion Laboratory, Pasadena, CA, <http://podaac.jpl.nasa.gov>).

## 3 Results

### 3.1 Distribution of surface $f\text{CO}_2$ observed in October and November

The KEOPS2 survey started in October, when surface chlorophyll *a* concentrations were still low in most of the studied area due to light limitation (Fig. 1a). As a consequence, surface  $f\text{CO}_2$  was close to equilibrium with atmospheric  $\text{CO}_2$  (388  $\mu\text{atm}$ ) or higher, with the exception of shallow coastal waters that acted as a large sink for atmospheric  $\text{CO}_2$ , with surface  $f\text{CO}_2$  values as low as 300  $\mu\text{atm}$  (Figs. 2a and 3a). South-east of Kerguelen Island, where the plateau deepens to more than 500 m, we observed a large region of  $\text{CO}_2$  outgassing ( $\Delta f\text{CO}_2$  around +20  $\mu\text{atm}$ ) associated with high surface salinity (Fig. 2e). High surface  $f\text{CO}_2$  values are representative of winter conditions in the Southern Ocean when vertical mixing maintains high concentrations of  $T\text{CO}_2$  in surface waters, therefore acting against the effect of cooling (e.g. Metzl et al., 2006). A smaller area of  $\text{CO}_2$  outgassing was also observed on the warm side of the Polar Front (PF) zone before the onset of the bloom. On the contrary, surface  $f\text{CO}_2$  measured in October on the cold side of (within) the PF meander was close to equilibrium with atmospheric  $\text{CO}_2$ .

Weekly satellite images of chlorophyll *a* show an early phytoplankton bloom in the warm waters of the PF zone east of 73° E at end of October. It was rapidly followed by an increase in chlorophyll *a* concentration in the cold waters over and downstream of the Plateau, such that early in November most of the study region acted as a sink for atmospheric  $\text{CO}_2$ , with surface  $f\text{CO}_2$  values ranging from 275 to 390  $\mu\text{atm}$ . The minimum and maximum  $f\text{CO}_2$  values were obtained in shallow waters (< 500 m). Very

BGD

11, 17543–17578, 2014

## Rapid establishment of the $\text{CO}_2$ sink

C. Lo Monaco et al.

Title Page

Abstract

Introduction

Conclusions

References

Tables

Figures

◀

▶

◀

▶

Back

Close

Full Screen / Esc

Printer-friendly Version

Interactive Discussion



**Rapid establishment  
of the CO<sub>2</sub> sink**

C. Lo Monaco et al.

Title Page

Abstract

Introduction

Conclusions

References

Tables

Figures

I◀

▶I

◀

▶

Back

Close

Full Screen / Esc

Printer-friendly Version

Interactive Discussion



low  $f\text{CO}_2$  values, down to  $100\ \mu\text{atm}$  below the atmospheric level, were also measured on the warm side of the PF zone (east of  $73.5^\circ\ \text{E}$ ), whereas within the PF meander ( $71$ – $73.5^\circ\ \text{E}$ ) the mean  $\Delta f\text{CO}_2$  was around  $-30\ \mu\text{atm}$ . The region over the Plateau south of Kerguelen Island, that acted as a source of  $\text{CO}_2$  in October, also turned into a relatively large sink in November, with  $\Delta f\text{CO}_2$  values ranging from  $-80$  to  $-30\ \mu\text{atm}$  (Figs. 2a and 3a).

In order to identify the mechanisms responsible for the evolution of surface  $f\text{CO}_2$  observed at the onset of the phytoplankton bloom, we analyzed in more details the underway surface measurements of  $f\text{CO}_2$  and other relevant parameters collected in different regions of the bloom. Below, we first present observations collected offshore (bathymetry  $> 1000\ \text{m}$ ) downstream of the Kerguelen Plateau, a region referred to as the Plume, and which includes the cold waters within the PF meander ( $71$ – $73.5^\circ\ \text{E}$ , hereafter the Middle zone), as well as the warmer waters found in the PF zone (north of  $47.4^\circ\ \text{S}$  and east of  $73.5^\circ\ \text{E}$ ). Next we present observations collected over the Plateau (iron source) south of the PF. We conclude the section by discussing the mean air–sea  $\text{CO}_2$  fluxes calculated in the different regions in October and November.

### 3.2 Evolution of surface $f\text{CO}_2$ in the plume

The survey downstream of the Kerguelen Plateau started on the 21 October, when chlorophyll  $a$  concentrations were still low and surface  $f\text{CO}_2$  was close to equilibrium with atmospheric  $\text{CO}_2$  (Figs. 1a and 2a, Table 1). Surface and water column measurements were collected along the north–south transect at  $\sim 72^\circ\ \text{E}$ , starting over the Plateau (station A3), covering the western part of the Plume (north of  $49.5^\circ\ \text{S}$ ), and crossing the Polar Front at his northernmost position ( $47.4^\circ\ \text{S}$ , Fig. 2). Surface  $f\text{CO}_2$  measurements obtained in the Plume show fluctuations around the equilibrium value with a maximum amplitude of  $45\ \mu\text{atm}$  (Fig. 3a). Because of low chlorophyll  $a$  concentrations, surface  $f\text{CO}_2$  is expected to vary with temperature and mixing. It is clear from Fig. 3 that the high surface  $f\text{CO}_2$  (small outgassing) observed between  $48$  and  $49^\circ\ \text{S}$  is related to high SST. However, less than half of the spatial variability in surface  $f\text{CO}_2$

**Rapid establishment  
of the CO<sub>2</sub> sink**

C. Lo Monaco et al.

[Title Page](#)[Abstract](#)[Introduction](#)[Conclusions](#)[References](#)[Tables](#)[Figures](#)[I◀](#)[▶I](#)[◀](#)[▶](#)[Back](#)[Close](#)[Full Screen / Esc](#)[Printer-friendly Version](#)[Interactive Discussion](#)

can be explained by the effect of temperature alone ( $\sim 15 \mu\text{atm } ^\circ\text{C}^{-1}$  according to Takahashi et al., 1993). Consequently, more than half of the observed variability is due to the higher  $T\text{CO}_2$  concentrations measured in the area of  $\text{CO}_2$  outgassing compared to the surrounding surface waters, which must be explained by lateral and/or vertical mixing. The rapid variations in SST observed within the PF meander reflect the re-circulation of southern (cold) and northern (warm) surface waters (Park et al., 2014). However, since the contribution of northern waters is expected to reduce surface  $T\text{CO}_2$  concentrations in the Plume compared to the cold southern waters, we conclude that lateral advection has a minor impact on surface  $f\text{CO}_2$  (due to the opposite effects of temperature and  $T\text{CO}_2$ ). Instead, our observations point to vertical mixing as the main driver for the observed spatial variations in surface  $f\text{CO}_2$ . Indeed, the  $\text{CO}_2$  outgassing observed between  $48$  and  $49^\circ \text{S}$  is related to relatively deep layers ( $80$ – $110 \text{m}$ ), while the small uptake of  $\text{CO}_2$  observed in the colder waters around  $49^\circ \text{S}$  (Fig. 3) can be attributed to the combined effect of reduced mixing ( $60$ – $70 \text{m}$ ) and low but significant chlorophyll  $a$  concentrations (Table 1).

The passage of the PF was marked by a rapid change in surface temperature from  $\sim 2.5$  to  $3.9^\circ\text{C}$  between  $47.5$  and  $47.4^\circ \text{S}$  (Figs. 2 and 3). This resulted in a rapid increase in surface  $f\text{CO}_2$  from near-equilibrium values south of the PF ( $387 \pm 7 \mu\text{atm}$ ) to a small source of  $\text{CO}_2$  north of the PF ( $406 \pm 12 \mu\text{atm}$ ), which can be explained by the temperature effect alone ( $+22 \mu\text{atm}$ ). In the warm waters of the PF zone, we recorded the maximum  $f\text{CO}_2$  value of  $430 \mu\text{atm}$  at  $47.3^\circ \text{S}$ , followed by a sudden decrease down to near-equilibrium, and a second  $f\text{CO}_2$  maximum at  $46.8^\circ \text{S}$  (Fig. 3a). Such rapid changes in surface  $f\text{CO}_2$  reflected the impact of mesoscale features associated with the frontal structure (Park et al., 2014).

The second visit of the Middle zone occurred 10 days later (31 October to 2 November) when both surface and water column measurements were collected along the east–west transect along  $\sim 48.5^\circ \text{S}$ . At that time the whole region had turned into a small sink for atmospheric  $\text{CO}_2$  of the order of  $10$  to  $20 \mu\text{atm}$  (Fig. 4a). This decrease in  $f\text{CO}_2$  resulted from the opposite effects of surface warming by  $\sim 0.7^\circ\text{C}$  ( $+11 \mu\text{atm}$ )

**Rapid establishment  
of the CO<sub>2</sub> sink**

C. Lo Monaco et al.

[Title Page](#)[Abstract](#)[Introduction](#)[Conclusions](#)[References](#)[Tables](#)[Figures](#)[I◀](#)[▶I](#)[◀](#)[▶](#)[Back](#)[Close](#)[Full Screen / Esc](#)[Printer-friendly Version](#)[Interactive Discussion](#)

and a decrease in  $TCO_2$  concentrations by  $\sim 10 \mu\text{mol kg}^{-1}$  (Table 1). The latter could partly be due to a small increase in chlorophyll *a* concentration observed over the 10 days period. Both the changes in  $TCO_2$  and chlorophyll *a* concentrations are likely related to the reduction in vertical mixing revealed by reduced mixed layer depths (40–90 m) and a decrease in surface salinity (Table 1). We observed a larger  $CO_2$  sink in the western (cold) part of the Plume ( $\sim 20 \mu\text{atm}$ ) compared to its eastern (warm) part ( $\sim 10 \mu\text{atm}$ ), which is explained by both temperature and  $TCO_2$  concentrations. The low surface  $fCO_2$  and  $TCO_2$  measured in cold waters were associated with high surface salinity and low  $Si(OH)_4$  concentrations, which could reflect an increased biological activity in the waters of southern origin (consistent with observations over the Plateau, see Sect. 3.3).

In the warm waters of the PF zone, the mixed layer was already relatively shallow at the end of October ( $< 80 \text{ m}$ , Table 2). Ten days later it was less than 40 m deep east of  $73.5^\circ \text{ E}$ , and a large area of intense biological uptake of  $CO_2$  was observed, with surface  $fCO_2$  values as low as  $290 \mu\text{atm}$  (Fig. 4a) and chlorophyll *a* concentrations between 2 and  $6 \mu\text{g L}^{-1}$  (Table 1). The reason for the early onset of an intense bloom in this area is not yet fully understood. One mechanism likely involved is the fast delivery of iron from the Plateau north of Kerguelen Island thanks to the strong jets associated with the frontal structure in this region (e.g., Lourantou and Metzl, 2011 ; Park et al., 2014), since we can expect that the amount of iron lost during the transit (due to biological and physical processes) is reduced. In the Middle region, the first important drawdown of  $fCO_2$  (down to  $350 \mu\text{atm}$ ) was observed on the 3 November over a small area ( $72.8\text{--}73^\circ \text{ E}$ ). Two days later, we measured a very similar  $CO_2$  sink at the same latitude, but covering a larger area ( $72.9\text{--}73.4^\circ \text{ E}$ ). This area was characterized by warmer SST ( $\sim 3.5^\circ \text{ C}$ ) than the surrounding waters ( $\sim 3.0^\circ \text{ C}$ , Fig. 4), which may reflect reduced vertical mixing and/or the incursion of warm waters from the PF zone.

By the 8 November most of the area investigated downstream of the Plateau acted as a moderate to large sink for atmospheric  $CO_2$ . In the Middle zone, the mean  $CO_2$  sink was of the order of  $30 \mu\text{atm}$ , and was associated with a doubling in chlorophyll *a* con-

centrations since the last visit three days before (Table 1). The effect of enhanced photosynthesis on surface  $f\text{CO}_2$  was partly compensated by a warming by  $\sim 0.3^\circ\text{C}$  on the eastern part of the Middle zone ( $72.5\text{--}73.6^\circ\text{E}$ ). The concomitance of surface warming and increased biological uptake of  $\text{CO}_2$  is attributed to reduced vertical mixing ( $< 80\text{ m}$ ). In the eastern part of the Plume, surface  $f\text{CO}_2$  remained low until the end of the survey, whereas large and rapid spatial variations were observed in surface  $f\text{CO}_2$  measured in the western part ( $71\text{--}72.5^\circ\text{E}$ , Fig. 4a). In the region between  $72$  and  $72.3^\circ\text{E}$ , where temperature remained relatively low all through November (around  $3^\circ\text{C}$ ), we observed an increase in surface  $f\text{CO}_2$  to near-equilibrium with atmospheric  $\text{CO}_2$  on the 10 November, followed by the re-establishment of the  $\text{CO}_2$  sink, and a second increase to near-equilibrium four days later. Similar changes in surface  $f\text{CO}_2$  were observed west of  $72^\circ\text{E}$ , but the driving mechanisms were somewhat different. Indeed, the increase to near-equilibrium observed on the 18 November was due to the combined effect of surface warming by  $\sim 0.5^\circ\text{C}$  (delayed by  $\sim 10$  days compared to the eastern part of the Plume) and reduced chlorophyll  $a$  concentrations (Table 1).

Low  $f\text{CO}_2$  values (down to  $320\ \mu\text{atm}$ ) were measured at the end of November where the PF reaches its northernmost position. These extreme values, however, were very localized. The mean  $f\text{CO}_2$  in the PF zone at the end of November was  $360\ \mu\text{atm}$ , with maximum values of  $380\ \mu\text{atm}$ .

### 3.3 Evolution of surface $\text{CO}_2$ over the Kerguelen Plateau

The southern part of the bloom, observed to the south-east of Kerguelen Island, where the Plateau deepens to  $500\text{--}1000\text{ m}$ , was investigated in details during the first KEOPS cruise in January–February 2005. These previous measurements, obtained during the declining phase of the bloom, showed a core of maximum chlorophyll  $a$  concentrations ( $> 1\ \mu\text{gL}^{-1}$ ) between  $50$  and  $51^\circ\text{S}$  at  $\sim 72^\circ\text{E}$  (station A3), associated with minimum surface  $f\text{CO}_2$  values ( $58 \pm 11\ \mu\text{atm}$  lower than in the surrounding HNLC waters, Blain et al., 2007). This area was revisited three times during the KEOPS2 survey (Table 1, Fig. 3).

BGD

11, 17543–17578, 2014

## Rapid establishment of the $\text{CO}_2$ sink

C. Lo Monaco et al.

Title Page

Abstract

Introduction

Conclusions

References

Tables

Figures

◀

▶

◀

▶

Back

Close

Full Screen / Esc

Printer-friendly Version

Interactive Discussion



**Rapid establishment  
of the CO<sub>2</sub> sink**

C. Lo Monaco et al.

Title Page

Abstract

Introduction

Conclusions

References

Tables

Figures



Back

Close

Full Screen / Esc

Printer-friendly Version

Interactive Discussion



In October, we measured high surface  $f\text{CO}_2$  in the Plateau region (50–51° S, 70–72° E), about 25  $\mu\text{atm}$  above atmospheric  $\text{CO}_2$ , whereas in HNLC waters upstream of the Plateau, surface  $f\text{CO}_2$  was near-equilibrium (Fig. 2a, Table 1). The  $\text{CO}_2$  outgassing observed over the Plateau is clearly related to the deep mixing observed in this area (MLD > 140 m, Fig. 2) compared to HNLC waters upstream (Table 2), leading to higher  $T\text{CO}_2$  and nutrients concentrations over the Plateau (Table 1). Surface temperature was slightly lower over the Plateau than in the waters upstream, and chlorophyll *a* concentration was slightly higher. This suggests that both temperature and primary production partly compensate for mixing with the  $\text{CO}_2$ -rich subsurface waters.

The combined effect of vertical mixing, temperature and photosynthesis on surface  $f\text{CO}_2$  was also observed between the first visit over the Plateau on the 18 October and the second visit on the following day, when the mean surface  $f\text{CO}_2$  was reduced by 13  $\mu\text{atm}$  and surface waters were cooler by  $\sim 0.2^\circ\text{C}$  (Fig. 3, Table 1). Sea surface cooling likely resulted from the low air temperature, combined with reduced vertical mixing, as suggested by water column measurements collected on the 20 October that showed an increase in temperature from the surface to the base of the mixed layer (by  $\sim 0.4^\circ\text{C}$ , Fig. 5). According to Takahashi et al. (1993), the temperature effect explains about 25 % of the sudden decrease in surface  $f\text{CO}_2$ . The remaining 75 % is attributed to enhanced photosynthesis. Indeed, water column measurements revealed that  $T\text{CO}_2$  concentrations were about 15  $\mu\text{mol kg}^{-1}$  lower at the surface than in the Winter Water layer found between 175 and 200 m (subsurface temperature minimum, Fig. 5). This signal supports the idea that the biological pump of  $\text{CO}_2$  was already active at the end of October, despite the deep mixed layer. This is further supported by a small increase in surface chlorophyll *a* concentrations observed between 18 and 21 October (Table 1), which may hide a larger increase in subsurface waters (chlorophyll maximum).

Surface measurements were collected three weeks later (8–9 November) in the northern part of the Plateau region (49.5–50° S, Fig. 3, Table 1). SST was higher than during the first visit ( $+0.5^\circ\text{C}$ ) due to warming in the atmosphere, and SSS was slightly lower, both suggesting reduced vertical mixing. Surface  $f\text{CO}_2$  decreased by  $\sim 90 \mu\text{atm}$

over the 3-weeks period, in response to an increase in chlorophyll *a* concentrations by a factor 10 ( $> 2 \mu\text{gL}^{-1}$ ) and possibly reduced mixing with subsurface waters. This resulted in a strong  $\text{CO}_2$  sink ( $\sim 60 \mu\text{atm}$ ) and minimum values in surface  $T\text{CO}_2$  and nutrients. At this time, when the bloom was growing, surface chlorophyll *a* concentrations were twice as large over the Plateau than in the Plume offshore, and the  $\text{CO}_2$  sink was twice as strong.

One week later (15–17 November), the last visit over the Plateau revealed an increase in surface  $f\text{CO}_2$  by  $\sim 25 \mu\text{atm}$  and reduced spatial variability (Fig. 3a), associated with sea surface cooling and mixed layers as deep as during the first occupation in October ( $\sim 150 \text{ m}$ , Table 2). The salinity profile was also very similar, while temperature increased by  $\sim 0.5 \text{ }^\circ\text{C}$  in the mixed layer due to warming in the atmosphere (Fig. 5). The concentration in chlorophyll *a* was quite homogeneous in the mixed layer, reflecting an effective mixing at the time of observation. This is supported by strong winds measured on the 15 November ( $15\text{--}20 \text{ ms}^{-1}$ ), and a rapid slow down on the following day ( $\sim 10 \text{ ms}^{-1}$ ). Our observations suggest that this short event of strong winds induced an increase in surface  $f\text{CO}_2$  of the order of  $30 \mu\text{atm}$ , followed by a decrease of about  $10 \mu\text{atm}$  when winds are reduced (although SST increased by  $\sim 0.2 \text{ }^\circ\text{C}$ ). Despite this deep mixing event, the Plateau region acted as a substantial sink for atmospheric  $\text{CO}_2$ , relatively steady at the end of the survey ( $39 \pm 6 \mu\text{atm}$ ), whereas in the Plume downstream of the Plateau, we observed large and rapid spatial and temporal variations in surface  $f\text{CO}_2$  resulting in a moderate  $\text{CO}_2$  sink at the end of the survey ( $26 \pm 10 \mu\text{atm}$ ).

### 3.4 Mean air–sea $\text{CO}_2$ fluxes in and out of Kerguelen’s bloom

Air–sea  $\text{CO}_2$  fluxes were generally small in October (Table 2). The largest flux was an outgassing of  $\text{CO}_2$  observed over the Plateau south of Kerguelen Island, which we attributed to deep mixing (140–180 m). Based on our observations, we can expect substantial variations in air–sea  $\text{CO}_2$  fluxes in this region due to rapid changes in winds and the subsequent stratification/destratification of the upper ocean. In the HNLC region upstream of the Plateau, we calculated a mean  $\text{CO}_2$  flux close to zero, associated

BGD

11, 17543–17578, 2014

## Rapid establishment of the $\text{CO}_2$ sink

C. Lo Monaco et al.

Title Page

Abstract

Introduction

Conclusions

References

Tables

Figures

◀

▶

◀

▶

Back

Close

Full Screen / Esc

Printer-friendly Version

Interactive Discussion



**Rapid establishment  
of the CO<sub>2</sub> sink**

C. Lo Monaco et al.

Title Page

Abstract

Introduction

Conclusions

References

Tables

Figures

I◀

▶I

◀

▶

Back

Close

Full Screen / Esc

Printer-friendly Version

Interactive Discussion



with shallower mixed layer (80–150 m). In the Middle zone, where the mixed layer was even shallower (60–110 m), the mean CO<sub>2</sub> flux was also close to zero before the onset of the bloom. This resulted from the combined effects of lateral and vertical mixing on SST and TCO<sub>2</sub> leading to a small outgassing of CO<sub>2</sub> in the warm waters, and low but significant biological activity that induced a small CO<sub>2</sub> sink in the cold waters of southern origin. In the PF zone, north of the plume, we estimated a small outgassing of CO<sub>2</sub> at the end of October, mainly explained by the temperature effect (warm waters). In shallow waters (< 500 m), our observations indicate a mean air–sea CO<sub>2</sub> flux close to zero in October, mostly due to small Δ*f*CO<sub>2</sub> values and the combination of CO<sub>2</sub> source (salty waters) and CO<sub>2</sub> sink areas. In the few places where we measured low *f*CO<sub>2</sub>, notably inside the Morbihan Gulf (SSS < 33.5, Fig. 2), the uptake of CO<sub>2</sub> was of the order of 30 mmolC m<sup>-2</sup> day<sup>-1</sup> for observed winds around 15 ms<sup>-1</sup>.

In November, the fertilized region over and downstream of the Plateau was globally a large sink for atmospheric CO<sub>2</sub>, as can be expected from chlorophyll *a* concentrations (Fig. 1). The largest uptake of atmospheric CO<sub>2</sub> was observed in the PF zone (~ 20 mmolC m<sup>-2</sup> day<sup>-1</sup>) and was associated with maximum chlorophyll *a* concentrations (Table 1). The mean CO<sub>2</sub> uptake estimated over the Plateau was twice as low than in the PF zone, but slightly larger than in the Middle zone (Table 2). However, the mean *f*CO<sub>2</sub> drawdown observed from October to November was three times larger over the Plateau (60 μatm) than in the Middle zone (20 μatm). We do not have observation in the PF zone east of 73.5° E before the onset of the bloom, but we can expect that surface *f*CO<sub>2</sub> was close to equilibrium with atmospheric CO<sub>2</sub> (similarly as what we observed in the PF zone north-east of Kerguelen Island and in the eastern part of the Middle zone). This would give a mean *f*CO<sub>2</sub> drawdown around 80 μatm, i.e., four times larger than in the Middle zone.

In shallow waters (bathymetry < 500 m), air–sea CO<sub>2</sub> fluxes were highly variable in November due to the large variability in surface *f*CO<sub>2</sub>. In coastal waters, the mean CO<sub>2</sub> uptake was as large as in the PF zone (~ 20 mmolC m<sup>-2</sup> day<sup>-1</sup>).

## 4 Discussion

Observations collected during the KEOPS2/OISO20 cruise have revealed differences in the mechanisms that control air–sea CO<sub>2</sub> fluxes in different regions of Kerguelen’s phytoplankton bloom. Over the southern Plateau, south of the PF, we observed rapid changes in surface *f*CO<sub>2</sub> due to changes in vertical mixing, both at the end of winter and during the productive season when strong winds events destratified the water column. Spatial variability, on the contrary, was reduced over the Plateau compared to the Middle zone. Due to the PF meander, the Middle zone could be seen as an incursion northward of cold waters enriched with *T*CO<sub>2</sub> and nutrients. The analysis of CTD, drifter and satellite data indeed suggests that cold waters are advected from the Plateau south of Kerguelen Island to the western (cold) part of the Middle region following the path of the PF (Park et al., 2014). North-East of Kerguelen Island, the PF meets the strong jets associated with the Subantarctic Front and turns eastward then southward. This allows mixing between warm waters enriched with iron (from their passage over the Plateau north of Kerguelen) and cold southern waters transported northward along the PF. The analysis of satellite data showed that the cold waters then get trapped in the cyclonic eddy observed around 72° E between 48 and 48.5° S. This structure is characterized by a minimum in chlorophyll *a* concentration within the bloom (Fig. 1b) and relatively low iron concentrations (Qu  rou   et al., 2014). The latter can be explained by the two circulation characteristics mentioned above: firstly the Middle region receive an inflow of HNLC waters from the passage in between the Kerguelen and Heard plateaus, and therefore not enriched by the iron sources located on shallow regions; secondly, part of the iron rich waters coming from the Plateau stagnates in the Middle zone for long times (~ 30 days or longer) so that their originally high iron content is depleted by biotic and abiotic scavenging mechanisms. On the contrary, the rapid transport of the waters from the Plateau North of Kerguelen, along the PF, allows for a larger input of iron in the northern and eastern parts of the Plume. This circulation pattern resulted in large

BGD

11, 17543–17578, 2014

### Rapid establishment of the CO<sub>2</sub> sink

C. Lo Monaco et al.

Title Page

Abstract

Introduction

Conclusions

References

Tables

Figures

◀

▶

◀

▶

Back

Close

Full Screen / Esc

Printer-friendly Version

Interactive Discussion



spatial gradients in the Plume for most surface properties, including temperature and chlorophyll *a*, hence  $f\text{CO}_2$ .

Due to light limitation, primary production was generally low in October despite the availability of nutrients, including iron over and downstream of the Plateau (Qu rou  et al., 2014). Consequently, surface  $f\text{CO}_2$  was mainly controlled by temperature and mixing. Figure 6a shows the relationship between surface  $f\text{CO}_2$  and temperature. In October we observed similar surface  $f\text{CO}_2$  values in the cold waters over the Plateau and in the warmest waters found in the PF zone to the north. Given the mean temperature difference, one could expect surface  $f\text{CO}_2$  to be 30  $\mu\text{atm}$  lower over the Plateau. This highlights the important contribution of vertical mixing in the control of winter air-sea  $\text{CO}_2$  fluxes. During the transport of cold waters from the Plateau to the Middle zone, surface  $f\text{CO}_2$  is reduced because of reduced vertical mixing and low primary production. Surface  $f\text{CO}_2$  is also slightly reduced when the warm waters of the PF zone are injected in the Middle zone (cooling effect). It follows that surface  $f\text{CO}_2$  was lower in the Middle zone than over the Plateau or in the PF zone, which illustrates the important role of re-circulation within the PF meander to generate a small uptake of atmospheric  $\text{CO}_2$  at the end of winter.

Our observations suggest that the start of the  $\text{CO}_2$  sink largely depends on vertical mixing due to both light limitation and mixing with subsurface waters. The stratification of the water column occurred between the end of October and the beginning of November. Over the Plateau, this first resulted in sea surface cooling (due to low air temperature) and a decrease in surface  $f\text{CO}_2$  by  $\sim 13 \mu\text{atm}$  due to the combined effects of cooling, reduced vertical mixing and photosynthesis. In the cold waters of the Middle zone, stratification was associated with sea surface warming, whose effect on surface  $f\text{CO}_2$  ( $+10 \mu\text{atm}$ ) played against the impact of reduced vertical mixing and photosynthesis, resulting in a small decrease in surface  $f\text{CO}_2$  (by  $\sim 10 \mu\text{atm}$ ), whereas in the warm waters of the Middle zone, SST did not change much, and surface  $f\text{CO}_2$  was thus reduced by  $\sim 20 \mu\text{atm}$ .

**BGD**

11, 17543–17578, 2014

## Rapid establishment of the $\text{CO}_2$ sink

C. Lo Monaco et al.

Title Page

Abstract

Introduction

Conclusions

References

Tables

Figures

◀

▶

◀

▶

Back

Close

Full Screen / Esc

Printer-friendly Version

Interactive Discussion



**Rapid establishment  
of the CO<sub>2</sub> sink**

C. Lo Monaco et al.

Title Page

Abstract

Introduction

Conclusions

References

Tables

Figures

I ◀

▶ I

◀

▶

Back

Close

Full Screen / Esc

Printer-friendly Version

Interactive Discussion



As soon as the mixed layer was reduced, we observed a significant increase in chlorophyll *a* concentrations over and downstream of the Plateau. The biological control on air–sea CO<sub>2</sub> fluxes can be appreciated through the relationship observed between surface *f*CO<sub>2</sub> and chlorophyll *a* concentrations, showing a good anti-correlation (both spatially and temporally) as soon as the bloom started to grow (Fig. 6b). We found differences in the magnitude of the CO<sub>2</sub> uptake in different regions of the bloom, which we attributed to biological activity and the availability of iron (small temperature effect). In the Middle zone (steady CO<sub>2</sub> sink of the order of  $-15 \mu\text{atm}$  at the end of winter), the onset of the bloom resulted in a mean *f*CO<sub>2</sub> drawdown of  $\sim 30 \mu\text{atm}$  in the eastern (warm) part and  $\sim 20 \mu\text{atm}$  in the western (cold) part. The latter was characterized by lower iron and chlorophyll *a* concentrations (hence higher surface *f*CO<sub>2</sub>) and rapid spatial and temporal variations in most surface properties due to movements of the cyclonic eddy observed around 72° E. The strongest CO<sub>2</sub> sink was observed in the PF zone east of Kerguelen Plateau, where the early stratification of the water column (probably at the end of October) led to an early and strong bloom. Assuming that surface *f*CO<sub>2</sub> was near equilibrium before the onset of the bloom, we estimated a mean *f*CO<sub>2</sub> drawdown of  $80 \mu\text{atm}$  for chlorophyll *a* concentrations exceeding  $2 \mu\text{g L}^{-1}$  (Fig. 6b), and attributed this large biological signal to the fast delivery of iron from the Plateau north of Kerguelen (strong jets). Our results thus suggest that once the ocean is stratified, the main mechanism controlling the magnitude of the CO<sub>2</sub> sink in the Plume offshore is lateral transport (pathway and speed).

Over the Plateau to the south, we observed a mean *f*CO<sub>2</sub> drawdown around  $60 \mu\text{atm}$  in response to the onset of the bloom for chlorophyll *a* concentrations between 2 and  $3 \mu\text{g L}^{-1}$  (Fig. 6b). Correcting for the increase in temperature that occurred after the stratification of the water column gives a mean biological signal around  $70 \mu\text{atm}$ . This number, obtained above the iron source, is fairly close to the biological signal estimated in the PF zone east of Kerguelen, two regions where iron was largely available at the beginning of the growing season (Quéroué et al., 2014). However, observations obtained at the end of the survey showed that the magnitude of the CO<sub>2</sub> sink over

**Rapid establishment  
of the CO<sub>2</sub> sink**

C. Lo Monaco et al.

[Title Page](#)[Abstract](#)[Introduction](#)[Conclusions](#)[References](#)[Tables](#)[Figures](#)[I ◀](#)[▶ I](#)[◀](#)[▶](#)[Back](#)[Close](#)[Full Screen / Esc](#)[Printer-friendly Version](#)[Interactive Discussion](#)

the Plateau can be substantially reduced (by  $\sim 25 \mu\text{atm}$ ) when the mixed layer deepens due to increased surface  $T\text{CO}_2$  concentrations (slightly counterbalanced by sea surface cooling). It is not clear whether reduced photosynthesis (light limitation) also contributed to enhance surface  $T\text{CO}_2$  because chlorophyll *a* concentration remained high (Fig. 6b). These results suggest that changes in winds and the following stratification/destratification of the upper ocean is another important factor (in addition to iron availability) in the control of air–sea  $\text{CO}_2$  fluxes over the Plateau (south of the PF).

As discussed before, the onset of the  $\text{CO}_2$  sink associated with Kerguelen's blooms seems to depend essentially on vertical mixing. The rapid  $f\text{CO}_2$  drawdown observed early in November (as soon as surface waters became isolated from the deep ocean) was clearly related to a decrease in surface  $T\text{CO}_2$  and nutrients concentrations due to both biological consumption in the upper layer and limited exchanges with the underlying deep reservoir. For this reason, we observed good relationships between surface  $f\text{CO}_2$  and the concentrations of major nutrients (Fig. 6c and d, Table 1). The largest reduction in surface nutrients was observed in the warm waters of the PF zone and over the Plateau to the south, where the biological uptake of  $\text{CO}_2$  was the largest. At the end of the survey, nitrate concentrations were still relatively high in all the regions investigated here ( $20\text{--}25 \mu\text{mol kg}^{-1}$ ), whereas silicic acid ( $\text{Si}(\text{OH})_4$ ) concentrations were of the order of  $10 \mu\text{mol kg}^{-1}$ , with the exception of the Plateau region where the deepening of the mixed layer refilled surface waters with nutrients (Table 1). In the course of the growing season, it is thus likely that  $\text{Si}(\text{OH})_4$  becomes rapidly depleted in the warm waters of the Plume, whereas  $\text{Si}(\text{OH})_4$  limitation is probably delayed in the cold waters over the Plateau thanks to higher winter concentrations and deep mixing events during summer. This hypothesis was supported by underway measurements collected three months later along the same east–west transect revisited during the next OISO cruise, and again one year later during the OISO22 cruise (February 2013). These re-occupations conducted later in the productive season showed a large reduction in chlorophyll *a* concentrations in the Plume offshore, which we attribute to the reduction in  $\text{Si}(\text{OH})_4$  concentrations. Indeed, maximum chlorophyll *a* concentrations ( $\sim 1 \mu\text{g L}^{-1}$ )

were observed in the cold waters transported northward along the PF ( $\sim 71^\circ$  E) where  $\text{Si}(\text{OH})_4$  concentrations were the highest ( $\sim 7 \mu\text{mol kg}^{-1}$ ), whereas in the Plume to the east ( $71.6\text{--}83^\circ$  E) chlorophyll *a* and  $\text{Si}(\text{OH})_4$  concentrations did not exceed  $0.2 \mu\text{g L}^{-1}$  and  $2 \mu\text{mol kg}^{-1}$  respectively.

Our results show that the magnitude of the  $\text{CO}_2$  sink at the start of the productive season mostly depends on iron availability. Because the Plateau is a source of iron, we estimated that the biological drawdown of  $\text{CO}_2$  was three times larger there than in the Middle (re-circulation) zone. As nutrients are consumed during the growing season, we propose that  $\text{Si}(\text{OH})_4$  eventually becomes depleted, thus replacing iron as limiting factor in regions where the upper ocean remains isolated from the underlying deep waters. Based on our observations, and assuming a delayed  $\text{Si}(\text{OH})_4$  depletion in cold waters, one might expect that the uptake of  $\text{CO}_2$  integrated over the whole productive season would be larger over the southern Plateau than in the Plume advected east of Kerguelen. In order to investigate this issue, we used the SOCAT database to draw the seasonal evolution of air–sea  $\text{CO}_2$  fluxes in the different regions of the bloom (Fig. 7). Surprisingly, the  $\text{CO}_2$  uptake integrated from October to March was similar over the Plateau and in the Middle zone ( $\sim 1 \text{ mol C m}^{-2}$ , Table 3), despite the large difference in the biological signal observed at the start of the productive season. The  $\text{CO}_2$  sink generally starts earlier in the Plume offshore (in October) than over the Plateau to the south (early in November, with only a few exception, for example in 2005 when a small  $\text{CO}_2$  sink was observed in October over the Plateau). The strongest  $\text{CO}_2$  uptake in the whole dataset is found in the PF zone at the onset of the bloom. However, observations obtained later in the season suggest that the  $\text{CO}_2$  sink is rapidly reduced by half, likely due to iron and/or  $\text{Si}(\text{OH})_4$  depletion. In the Middle zone and over the Plateau to the south, the decline of the  $\text{CO}_2$  sink is delayed by one or two months, likely due to the delayed nutrients depletion that can be explained by a lower biological consumption in the Middle zone and the refill of surface waters during deep mixing events over the Plateau. The data collected during the declining phase of the bloom (from January to March) show a faster decrease in the  $\text{CO}_2$  uptake over the Plateau than in the Middle

## Rapid establishment of the $\text{CO}_2$ sink

C. Lo Monaco et al.

[Title Page](#)[Abstract](#)[Introduction](#)[Conclusions](#)[References](#)[Tables](#)[Figures](#)[I◀](#)[▶I](#)[◀](#)[▶](#)[Back](#)[Close](#)[Full Screen / Esc](#)[Printer-friendly Version](#)[Interactive Discussion](#)

zone, which can be explained by vertical mixing, similarly as for the onset of the CO<sub>2</sub> sink in October/November.

In contrast to the bloom region, air–sea CO<sub>2</sub> fluxes show no clear seasonal cycle in HNLC waters (Fig. 7). The mean flux calculated in January agrees well with the value of  $-1.1 \text{ mmol C m}^{-2} \text{ day}^{-1}$  estimated by Metzl et al. (2006) based on data collected upstream of the Kerguelen Plateau ( $\sim 65^\circ \text{ E}$ ,  $50\text{--}58^\circ \text{ S}$ ). In August, they reported a small CO<sub>2</sub> outgassing in this region ( $+2.5 \text{ mmol C m}^{-2} \text{ day}^{-1}$ ), whereas we estimated a small CO<sub>2</sub> sink. Consequently, their estimate of the annual CO<sub>2</sub> uptake ( $0.5 \text{ mmol C m}^{-2}$ ) is lower than ours ( $0.8 \text{ mmol C m}^{-2}$ ).

## 5 Conclusions

The KEOPS2/OISO20 cruise allowed to monitor the establishment of the CO<sub>2</sub> sink associated with Kerguelen phytoplankton bloom, and to investigate the mechanisms that control air–sea CO<sub>2</sub> fluxes at the start of the productive season. Observations obtained in October support the idea that winter deep mixing plays a key role in limiting the uptake of atmospheric CO<sub>2</sub> in the Southern Ocean, both because of light limitation and mixing with the CO<sub>2</sub>-rich subsurface waters. We found that the temperature effect on  $f\text{CO}_2$  is generally small south of the PF, while in the PF zone, reduced mixing at the end of winter is associated with sea surface warming that would maintain high surface  $f\text{CO}_2$  if primary production did not increase. Stratification of the upper ocean marks the start of the growing season and is rapidly followed by the establishment of a strong CO<sub>2</sub> sink over and downstream the Kerguelen Plateau. Our results show that the magnitude of the CO<sub>2</sub> sink at the start of the productive season is closely related to chlorophyll *a* concentration and iron availability. In the Plume, iron availability strongly depends on lateral advection that transports iron from the remote sources: either from north of the island to the eastern part of the Plume (fast delivery due to the strong jets), or from the south to the western part of the Plume (mixing with HNLC waters, recirculation). Lateral transport is thus identified as the main mechanism explaining the

Title Page

Abstract

Introduction

Conclusions

References

Tables

Figures

⏪

⏩

◀

▶

Back

Close

Full Screen / Esc

Printer-friendly Version

Interactive Discussion



**Rapid establishment  
of the CO<sub>2</sub> sink**

C. Lo Monaco et al.

[Title Page](#)[Abstract](#)[Introduction](#)[Conclusions](#)[References](#)[Tables](#)[Figures](#)[I ◀](#)[▶ I](#)[◀](#)[▶](#)[Back](#)[Close](#)[Full Screen / Esc](#)[Printer-friendly Version](#)[Interactive Discussion](#)

moderate uptake of atmospheric CO<sub>2</sub> observed in the Plume in November. Over the Plateau (iron source), we observed a larger and spatially more homogeneous CO<sub>2</sub> sink. Nevertheless, we also observed an episode of deep mixing (~ 150 m) over the Plateau after the onset of the bloom, which resulted in a substantial reduction in the uptake of atmospheric CO<sub>2</sub> due to increased surface TCO<sub>2</sub> concentrations. Such episodic destratification of the water column could explain why the uptake of CO<sub>2</sub> integrated over the productive season was similar over the Plateau and in the Plume offshore, despite the delayed depletion in Si(OH)<sub>4</sub> and iron over the Plateau. Using all available information, we estimated an uptake of CO<sub>2</sub> between 1 and 1.5 mol C m<sup>-2</sup> in the bloom area when integrated over the productive season (October to March), which is between 2.5 and 4 times larger than value estimated in HNLC waters. Extrapolating our results to the whole Permanent Open Ocean Zone between 50 and 60° S (~ 9.10<sup>6</sup> km<sup>2</sup>, Metzl et al., 2006) suggests that if this region was fertilized with iron in the same manner as what we observed around Kerguelen, the annual uptake of atmospheric CO<sub>2</sub> would increase by less than 0.1 Pg of carbon. We thus conclude that although iron fertilization in the Southern Ocean rapidly activates the biological uptake of CO<sub>2</sub>, its impact on the global carbon budget is very likely negligible compared to the 10 Pg of anthropogenic carbon released every year to the atmosphere (Le Quéré et al., 2014).

*Acknowledgements.* We thank S. Blain, project leader, and B. Quéguiner, chief scientist, as well as the captain and crew of R.R.V. *Marion Dufresne* and the staff at the French Polar Institute (IPEV) for their important contribution to the success of the cruise. We are also very grateful to all technicians and scientists who helped to obtain and interpret our data, in particular J. Capparos, L. Chirurgien, C. De La Vega, I. Durand, A. Guéneuguès, F. Kaczmar, D. Lefevre, L. Merlivat, L. Oriol, and F. Perrault. The KEOPS2 project was funded by the French institutes INSU (Institut National des Sciences de l'Univers), IPEV (Institut Paul Emile Victor) and ANR (Agence Nationale de la Recherche). The OISO program is supported by the French institutes INSU, IPEV and IPSL (Institut Pierre Simon Laplace), and the European project FP7/CARBOCHANGE (grant 264879).

## References

- Bakker, D. C. E., Nielsdottir, M. C., Morris, P. J., Venables, H. J., and Watson, A. J.: The island mass effect and biological carbon uptake for the subantarctic Crozet Archipelago, *Deep-Sea Res. Pt. II*, 54, 2174–2190, 2007.
- 5 Bakker, D. C. E., Pfeil, B., Smith, K., Hankin, S., Olsen, A., Alin, S. R., Cosca, C., Harasawa, S., Kozyr, A., Nojiri, Y., O'Brien, K. M., Schuster, U., Telszewski, M., Tilbrook, B., Wada, C., Aki, J., Barbero, L., Bates, N. R., Boutin, J., Bozec, Y., Cai, W.-J., Castle, R. D., Chavez, F. P., Chen, L., Chierici, M., Currie, K., de Baar, H. J. W., Evans, W., Feely, R. A., Fransson, A., Gao, Z., Hales, B., Hardman-Mountford, N. J., Hoppema, M., Huang, W.-J., Hunt, C. W.,  
10 Huss, B., Ichikawa, T., Johannessen, T., Jones, E. M., Jones, S. D., Jutterström, S., Kitidis, V., Körtzinger, A., Landschützer, P., Lauvset, S. K., Lefèvre, N., Manke, A. B., Mathis, J. T., Merlivat, L., Metzl, N., Murata, A., Newberger, T., Omar, A. M., Ono, T., Park, G.-H., Pater-son, K., Pierrot, D., Ríos, A. F., Sabine, C. L., Saito, S., Salisbury, J., Sarma, V. V. S. S., Schlitzer, R., Sieger, R., Skjelvan, I., Steinhoff, T., Sullivan, K. F., Sun, H., Sutton, A. J.,  
15 Suzuki, T., Sweeney, C., Takahashi, T., Tjiputra, J., Tsurushima, N., van Heuven, S. M. A. C., Vandemark, D., Vlahos, P., Wallace, D. W. R., Wanninkhof, R., and Watson, A. J.: An up-  
date to the Surface Ocean CO<sub>2</sub> Atlas (SOCAT version 2), *Earth Syst. Sci. Data*, 6, 69–90, doi:10.5194/essd-6-69-2014, 2014.
- Blain, S., Quéguiner, B., Armand, L., Belviso, S., Bombled, B., Bopp, L., Bowie, A., Brunet, C.,  
20 Brussaard, C., Carlotti, F., Christaki, U., Corbière, A., Durand, I., Ebersbach, F., Fuda, J.-L., Garcia, N., Gerringa, L., Griffiths, B., Guigue, C., Guillerm, C., Jacquet, S., Jeandel, C., Laan, P., Lefèvre, D., Lomonaco, C., Malits, A., Mosseri, J., Obernosterer, I., Park, Y.-H., Picheral, M., Pondaven, P., Remeny, T., Sandroni, V., Sarthou, G., Savoye, N., Scouarnec, L., Souhaut, M., Thuiller, D., Timmermans, K., Trull, T., Uitz, J., van-Beek, P., Veldhuis, M.,  
25 Vincent, D., Viollier, E., Vong, L., and Wagener, T.: Effect of natural iron fertilization on carbon sequestration in the Southern Ocean, *Nature*, 446, 1070–1074, doi:10.1038/nature05700, 2007.
- Blain, S., Capparos, J., Guéneuguès, A., Obernosterer, I., and Oriol, L.: Distributions and sto-  
30 iochimetry of dissolved nitrogen and phosphorus in the iron fertilized region near Kerguelen (Southern Ocean), *Biogeosciences Discuss.*, 11, 9949–9977, doi:10.5194/bgd-11-9949-2014, 2014.

### Rapid establishment of the CO<sub>2</sub> sink

C. Lo Monaco et al.

Title Page

Abstract

Introduction

Conclusions

References

Tables

Figures



Back

Close

Full Screen / Esc

Printer-friendly Version

Interactive Discussion



## Rapid establishment of the CO<sub>2</sub> sink

C. Lo Monaco et al.

Title Page

Abstract

Introduction

Conclusions

References

Tables

Figures

◀

▶

◀

▶

Back

Close

Full Screen / Esc

Printer-friendly Version

Interactive Discussion



Boyd, P. W., Law, C. S., Wong, C. S., Nojiri, Y., Tsuda, A., Levasseur, M., Takeda, S., Rivkin, R., Harrison, P. J., Strzepek, R., Gower, J., McKay, R. M., Abraham, E., Arychuk, M., BarwellClarke, J., Crawford, W., Crawford, D., Hale, M., Harada, K., Johnson, K., Kiyosawa, H., Kudo, I., Marchetti, A., Miller, W., Needoba, J., Nishioka, J., Ogawa, H., Page, J., Robert, M., Saito, H., Sastri, A., Sherry, N., Soutar, T., Sutherland, N., Taira, Y., Whitney, F., Wong, S. K. E., and Yoshimura, T.: Mesoscale iron enrichment experiments 1993–2005: synthesis and future directions, *Science*, 315, 612–617, doi:10.1126/science.1131669, 2007.

Jabaud-Jan, A., Metzl, N., Brunet, C., Poisson, A., and Schauer, B.: Variability of the carbon dioxide system in the southern Indian Ocean (20° S–60° S): the impact of a warm anomaly in austral summer 1998, *Global Biogeochem. Cy.*, 18, GB1042, doi:10.1029/2002GB002017, 2004.

Jouandet, M. P., Blain, S., Metzl, N., Brunet, C., Trull, T. W., and Obernosterer, I.: A seasonal carbon budget for a naturally iron-fertilized bloom over the Kerguelen Plateau in the Southern Ocean, *Deep-Sea Res. Pt. II*, 55, 856–867, doi:10.1016/j.dsr2.2007.12.037, 2008.

Le Quéré, C., Peters, G. P., Andres, R. J., Andrew, R. M., Boden, T. A., Ciais, P., Friedlingstein, P., Houghton, R. A., Marland, G., Moriarty, R., Sitch, S., Tans, P., Arneeth, A., Arvanitis, A., Bakker, D. C. E., Bopp, L., Canadell, J. G., Chini, L. P., Doney, S. C., Harper, A., Harris, I., House, J. I., Jain, A. K., Jones, S. D., Kato, E., Keeling, R. F., Klein Goldewijk, K., Körtzinger, A., Koven, C., Lefèvre, N., Maignan, F., Omar, A., Ono, T., Park, G.-H., Pfeil, B., Poulter, B., Raupach, M. R., Regnier, P., Rödenbeck, C., Saito, S., Schwinger, J., Segschneider, J., Stocker, B. D., Takahashi, T., Tilbrook, B., van Heuven, S., Viovy, N., Wanninkhof, R., Wiltshire, A., and Zaehle, S.: Global carbon budget 2013, *Earth Syst. Sci. Data*, 6, 235–263, doi:10.5194/essd-6-235-2014, 2014.

Lenton, A., Tilbrook, B., Law, R. M., Bakker, D., Doney, S. C., Gruber, N., Ishii, M., Hoppema, M., Lovenduski, N. S., Matear, R. J., McNeil, B. I., Metzl, N., Mikaloff Fletcher, S. E., Monteiro, P. M. S., Rödenbeck, C., Sweeney, C., and Takahashi, T.: Sea–air CO<sub>2</sub> fluxes in the Southern Ocean for the period 1990–2009, *Biogeosciences*, 10, 4037–4054, doi:10.5194/bg-10-4037-2013, 2013.

Lourantou, A. and Metzl, N.: Decadal evolution of carbon sink within a strong bloom area in the subantarctic zone, *Geophys. Res. Lett.*, 38, L23608, doi:10.1029/2011GL049614, 2011.

Martin, J. H., Gordon, R. M., and Fitzwater, S. E.: Iron in Antarctic waters, *Nature*, 345, 156–158, 1990.

**Rapid establishment  
of the CO<sub>2</sub> sink**

C. Lo Monaco et al.

Title Page

Abstract

Introduction

Conclusions

References

Tables

Figures

I ◀

▶ I

◀

▶

Back

Close

Full Screen / Esc

Printer-friendly Version

Interactive Discussion



- Metzl, N.: Decadal increase of oceanic carbon dioxide in southern Indian Ocean surface waters (1991–2007), *Deep-Sea Res. Pt. II*, 56, 607–619, 2009.
- Metzl, N., Poisson, A., Louanchi, F., Brunet, C., Schauer, B., and Brès, B.: Spatio-temporal distributions of air–sea fluxes of CO<sub>2</sub> in the Indian and Antarctic Oceans: a first step, *Tellus B*, 47, 56–69, 1995.
- Metzl, N., Tilbrook, B., and Poisson, A.: The annual *f*CO<sub>2</sub> cycle and the air–sea CO<sub>2</sub> flux in the sub-Antarctic Ocean, *Tellus B*, 51, 849–861, 1999.
- Metzl, N., Brunet, C., Jabaud-Jan, A., Poisson, A., and Schauer, B.: Summer and winter air–sea CO<sub>2</sub> fluxes in the Southern Ocean, *Deep-Sea Res. Pt. I*, 53, 1548–1563, doi:10.1016/j.dsr.2006.07.006, 2006.
- Mongin, M., Molina, E., and Trull, T. W.: Seasonality and scale of the Kerguelen plateau phytoplankton bloom: a remote sensing and modeling analysis of the influence of natural iron fertilization in the Southern Ocean, *Deep-Sea Res. Pt. II*, 55, 880–892, doi:10.1016/j.dsr2.2007.12.039, 2008.
- Neveux, J. and Lantoiné, F.: Spectrofluorometric assay of chlorophylls and phaeopigments using the least squares approximation technique, *Deep-Sea Res. Pt. I*, 40, 1747–1765, 1993.
- Park, Y.-H., Durand, I., Kestenare, E., Rougier, G., Zhou, M., d'Ovidio, F., Cotté, C., and Lee, J.-H.: Polar Front around the Kerguelen Islands: an up-to-date determination and associated circulation of surface/subsurface waters, *J. Geophys. Res.-Oceans*, 119, 6575–6592, doi:10.1002/2014JC010061, 2014.
- Poisson, A., Metzl, N., Brunet, C., Schauer, B., Brès, B., Ruiz-Pino, D., and Louanchi, F.: Variability of sources and sinks of CO<sub>2</sub> and in the western Indian and Southern Oceans during the year 1991, *J. Geophys. Res.*, 98, 22759–22778, 1993.
- Quéroué, F., Sarthou, G., Chever, F., van der Merwe, P., Lannuzel, D., Townsend, A., Bucciarelli, E., Planquette, H., Cheize, M., Blain, S., D'Ovidio, F., and Bowie, A.: A new study of natural Fe fertilization processes in the vicinity of the Kerguelen Islands (KEOPS2 experiment), *Biogeosciences Discuss.*, 2014.
- Schlitzer, R.: Ocean Data View, available at: <http://odv.awi.de> (last access: September 2014), 2014.
- Tagliabue, A., Mtshali, T., Aumont, O., Bowie, A. R., Klunder, M. B., Roychoudhury, A. N., and Swart, S.: A global compilation of dissolved iron measurements: focus on distributions and processes in the Southern Ocean, *Biogeosciences*, 9, 2333–2349, doi:10.5194/bg-9-2333-2012, 2012.

Takahashi, T., Olafsson, J., Goddard, J., Chipman, D. W., and Sutherland, S. C.: Seasonal variation of CO<sub>2</sub> and nutrients in the high-latitude surface oceans: a comparative study, *Global Biogeochem. Cy.*, 7, 843–878, 1993.

5 Takahashi, T., Sutherland, S. C., Wanninkhof, R., Sweeney, C., Feely, R. A., Chipman, D. W., Hales, B., Friederich, G., Chavez, F., Sabine, C., Watson, A., Bakker, D. C. E., Schuster, U., Metzl, N., Yoshikawa-Inoue, H., Ishii, M., Midorikawa, T., Nojiri, Y., Kortzinger, A., Steinhoff, T., Hoppema, M., Olafsson, J., Arnarson, T. S., Tillbrook, B., Johannessen, T. and Olsen, A., Bellerby, R., Wong, C. S., Delille, B., Bates, N. R., and de Baar, H. J. W.: Climatological mean and decadal change in surface ocean pCO<sub>2</sub>, and net sea–air CO<sub>2</sub> flux over the global oceans, *Deep-Sea Res. Pt. II*, 56, 554–577, doi:10.1016/j.dsr2.2008.12.009, 2009.

10 Wanninkhof, R.: Relationship between wind speed and gas exchange over the ocean, *J. Geophys. Res.*, 97, 7373–7382, doi:10.1029/92JC00188, 1992.

Weiss, R. F.: Carbon dioxide in water and seawater: the solubility of a non-ideal gas, *Mar. Chem.*, 2, 203–215, doi:10.1016/0304-4203(74)90015-2, 1974.

**BGD**

11, 17543–17578, 2014

---

## Rapid establishment of the CO<sub>2</sub> sink

C. Lo Monaco et al.

---

Title Page

Abstract

Introduction

Conclusions

References

Tables

Figures

◀

▶

◀

▶

Back

Close

Full Screen / Esc

Printer-friendly Version

Interactive Discussion





## Rapid establishment of the CO<sub>2</sub> sink

C. Lo Monaco et al.

**Table 2.** Mean  $\Delta f\text{CO}_2$  (sea–air), wind speed, air–sea CO<sub>2</sub> fluxes and range of the mixed layer depth (MLD) observed in October and November 2011 around Kerguelen.

	Month	$\Delta f\text{CO}_2$ ( $\mu\text{atm}$ )	Wind speed ( $\text{ms}^{-1}$ )	CO <sub>2</sub> flux ( $\text{mmolm}^{-2}\text{d}^{-1}$ )		MLD range (m)
				obs.wind <sup>a</sup>	clim.wind <sup>a</sup>	
Upstream (HNLC)	Oct	$-3 \pm 12$	$7 \pm 4$	-0.3	-0.8	80–150
Plateau (500–1000 m)	Oct	$17 \pm 9$	$14 \pm 3$	+7.2	+4.8	140–180
Plateau (500–1000 m)	Nov	$-44 \pm 13$	$10 \pm 4$	-9.5	-12.4	40–170
Middle zone	Oct	$-7 \pm 11$	$11 \pm 4$	-1.8	-2.1	60–110
Middle zone	Nov	$-27 \pm 11$	$13 \pm 4$	-9.6	-7.4	20–90
PF zone ( $\sim 47^\circ\text{S}$ )	Oct	$18 \pm 12$	$4 \pm 1$	+0.7	+4.9	40–80
PF zone ( $> 73.5^\circ\text{E}$ )	Nov	$-77 \pm 23$	$11 \pm 5$	-17.9	-21.2	20–40
Shallow Plateau (< 500 m)	Oct	$4 \pm 15$	$9 \pm 5$	+0.7	+1.0	20–40
Shallow Plateau (< 500 m)	Nov	$-33 \pm 33$	$17 \pm 3$	-19.3	-9.2	25

<sup>a</sup>CO<sub>2</sub> fluxes are calculated using either observed winds or the climatological value of  $11.5\text{ms}^{-1}$ .

Title Page

Abstract

Introduction

Conclusions

References

Tables

Figures

◀

▶

◀

▶

Back

Close

Full Screen / Esc

Printer-friendly Version

Interactive Discussion



## Rapid establishment of the CO<sub>2</sub> sink

C. Lo Monaco et al.

Title Page

Abstract

Introduction

Conclusions

References

Tables

Figures

◀

▶

◀

▶

Back

Close

Full Screen / Esc

Printer-friendly Version

Interactive Discussion



**Table 3.** Climatological wind speed and air–sea CO<sub>2</sub> fluxes.

	Winds (ms <sup>-1</sup> )	Air–sea CO <sub>2</sub> fluxes (monthly means in mmol C m <sup>-2</sup> day <sup>-1</sup> )			
		HNLC (0–160° E)	Plateau	Middle zone	PF zone
Aug	12.5 ± 1.1	-0.7 ± 3.0	6.3 ± 2.6	N.D. <sup>a</sup>	2.8 ± 3.2
Sep	12.1 ± 0.5	-2.1 ± 2.1	5.4 ± 3.1	3.1 ± 1.0	4.4 ± 2.4
Oct	11.5 ± 0.7	-2.2 ± 2.5	3.5 ± 2.9	-0.3 ± 2.0	-0.3 ± 2.9
Nov	10.8 ± 0.8	-2.2 ± 1.2	-9.5 ± 1.5	-7.2 ± 4.5	-18.7 ± 3.6
Dec	10.2 ± 0.9	-2.8 ± 2.4	N.D. <sup>a</sup>	-10 <sup>b</sup>	-8 ± 5.7
Jan	10.6 ± 0.8	-2.3 ± 2.8	-12 ± 5.4	-8.8 ± 2.1	-7.9 ± 5.6
Feb	10.3 ± 0.7	-1.3 ± 2.6	-7.9 ± 5.2	-7.5 ± 3.3	-8.6 ± 5.8
Mar	10.6 ± 0.7	-2.1 ± 1.6	3.0 ± 2.9	-2.6 ± 0.7	N.D. <sup>a</sup>
Apr	11.2 ± 0.8	-4.1 ± 2.8	N.D. <sup>a</sup>	N.D. <sup>a</sup>	-8 ± 2.8
May	11.8 ± 1.0	-4.0 ± 2.3	N.D. <sup>a</sup>	N.D. <sup>a</sup>	-0.7 ± 1.3
Jun	11.3 ± 1.2	-0.8 ± 0.5	N.D. <sup>a</sup>	N.D. <sup>a</sup>	1.4 ± 0.9
Jul	12.3 ± 0.7	-1.6 ± 1.3	N.D. <sup>a</sup>	N.D. <sup>a</sup>	-0.9 ± 3
		Integrated air–sea CO <sub>2</sub> fluxes (mmol C m <sup>-2</sup> )			
Oct to Mar		-394	-1008 <sup>c</sup>	-1095	-1550 <sup>d</sup>
Annual uptake		-798			-1581 <sup>d</sup>

<sup>a</sup>No Data;

<sup>b</sup>calculated from CARIOCA buoy *f*CO<sub>2</sub> data;

<sup>c</sup>calculated assuming a mean flux of -10.7 mmol C m<sup>-2</sup> day<sup>-1</sup> in December;

<sup>d</sup>calculated assuming a mean flux of -8.3 mmol C m<sup>-2</sup> day<sup>-1</sup> in March.

**Rapid establishment  
of the CO<sub>2</sub> sink**

C. Lo Monaco et al.

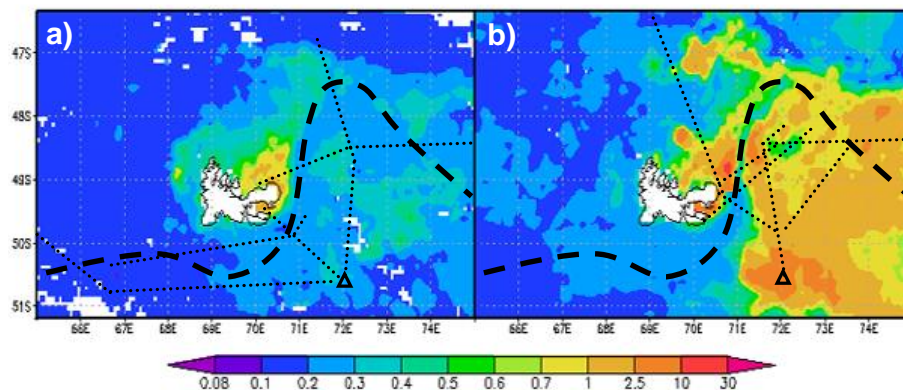


**Figure 1.** Satellite images of chlorophyll *a* ( $\mu\text{g L}^{-1}$ ) for **(a)** October 2011 and **(b)** November 2011 (MODIS, monthly mean). Dotted lines indicates the cruise track (the triangle locates station A3). The dashed line shows the mean position of the Polar Front (from Park et al., 2014).

[Title Page](#)[Abstract](#)[Introduction](#)[Conclusions](#)[References](#)[Tables](#)[Figures](#)[I ◀](#)[▶ I](#)[◀](#)[▶](#)[Back](#)[Close](#)[Full Screen / Esc](#)[Printer-friendly Version](#)[Interactive Discussion](#)

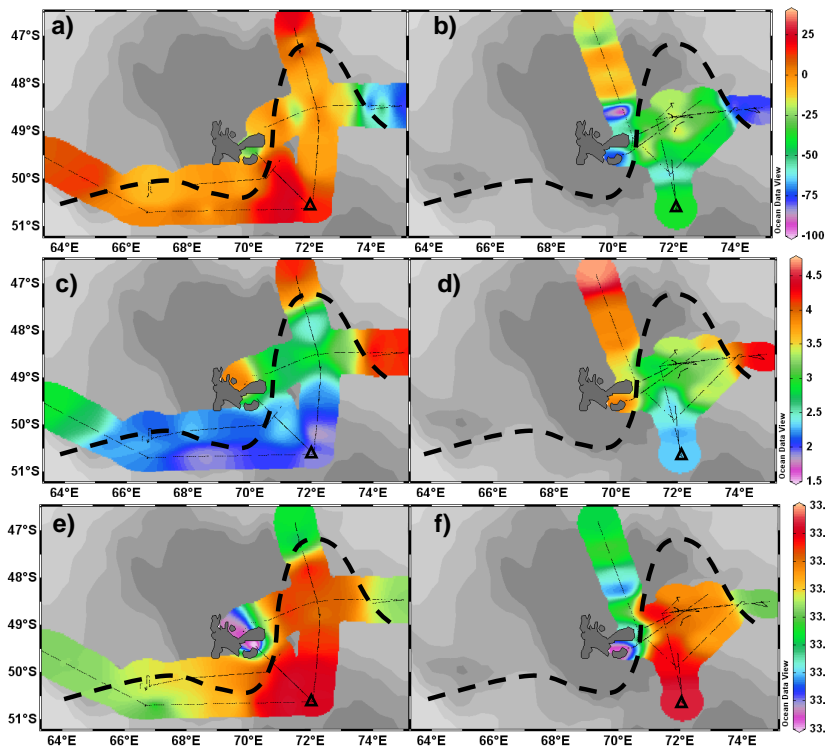


**Figure 2.** Underway surface measurements of (a and b)  $\Delta f\text{CO}_2$  (sea–air, in  $\mu\text{atm}$ ), (c and d) temperature ( $^{\circ}\text{C}$ ) and (e and f) salinity obtained during the winter to summer transition in 2011. Left panels show observations collected in October and early November (17 October–5 November), while right panels show observations obtained exclusively in November (5–21 November). Thin dotted lines indicates the cruise track (the triangle locates station A3). The dashed line shows the mean position of the Polar Front (from Park et al., 2014). Bathymetry is indicated as shades of grey (every 500 m).

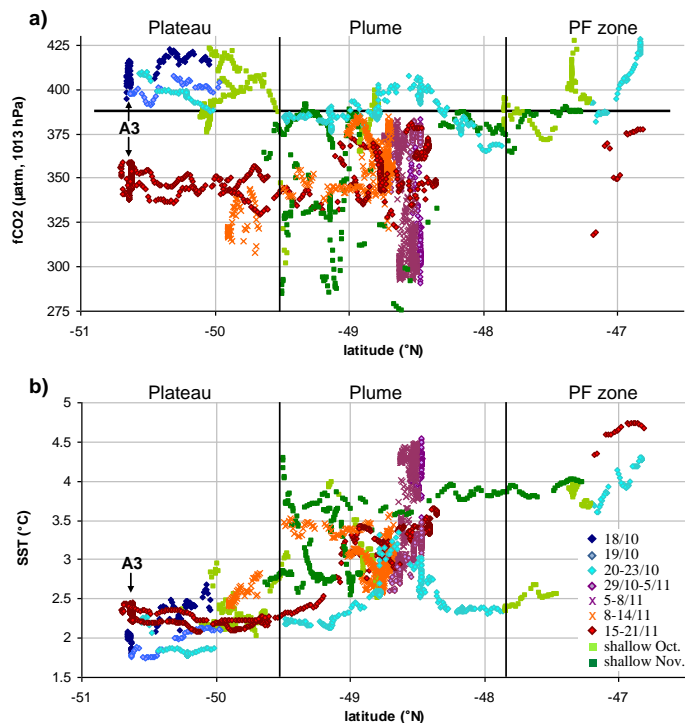


**Figure 3.** North–South distribution of **(a)** surface  $f\text{CO}_2$  and **(b)** sea surface temperature measured in October–November 2011 over and downstream of the Kerguelen Plateau (66.6–75° E). Symbols and color coding are used to indicate the time of observation: blue colors indicate end-winter conditions; purple symbols show the onset of the bloom; orange and red symbols are for mid-November. Green squares show measurements collected in shallow waters (bathymetry < 500 m) in October and November. The black horizontal line indicates the mean atmospheric  $f\text{CO}_2$  value of 388  $\mu\text{atm}$ . The position of station A3 is indicated (see profiles in Fig. 5).

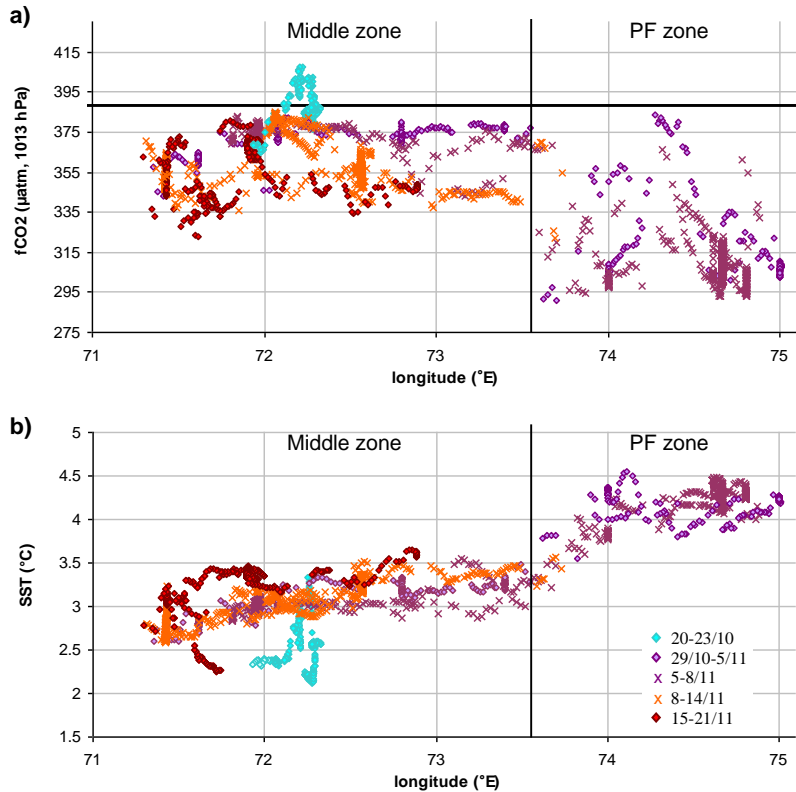


**Figure 4.** East–West distribution of **(a)** surface  $f\text{CO}_2$  and **(b)** sea surface temperature measured in October–November 2011 in the Plume offshore (47.8–49.5° S, bathymetry > 1000 m). Symbols and color coding are used to indicate the time of observation (same coding as for Fig. 3): blue dots indicate end-winter conditions; purple symbols show the onset of the bloom; orange and red symbols are for mid-November. The black horizontal line indicates the mean atmospheric  $f\text{CO}_2$  value of 388  $\mu\text{atm}$ .

## Rapid establishment of the CO<sub>2</sub> sink

C. Lo Monaco et al.

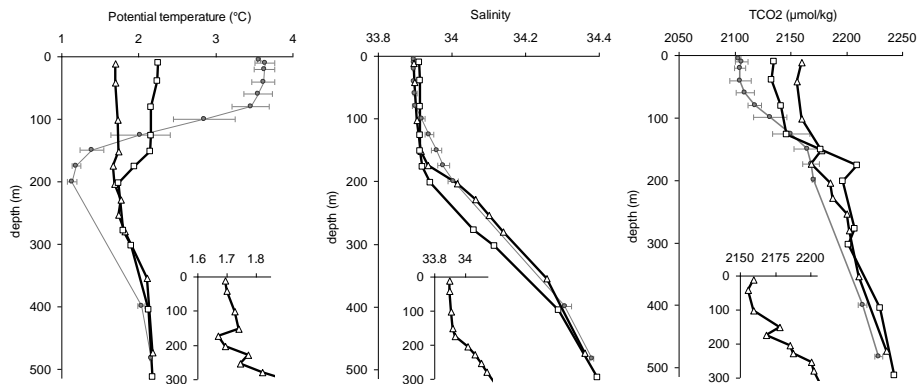


**Figure 5.** Vertical profiles of **(a)** potential temperature, **(b)** salinity and **(c)** total CO<sub>2</sub> measured at station A3 during the KEOPS2 survey in 2011 (black) before the onset of the bloom (20 October, triangles, with a zoom between 0 and 300 m) and during the growing season (16 November, squares), compared to the mean and SD of measurements collected during the KEOPS/OISO12 survey in 2005 when the bloom declined (19 January–12 February, gray dots, Jouandet et al., 2008).

Title Page

Abstract

Introduction

Conclusions

References

Tables

Figures

◀

▶

◀

▶

Back

Close

Full Screen / Esc

Printer-friendly Version

Interactive Discussion





Rapid establishment  
of the CO<sub>2</sub> sink

C. Lo Monaco et al.

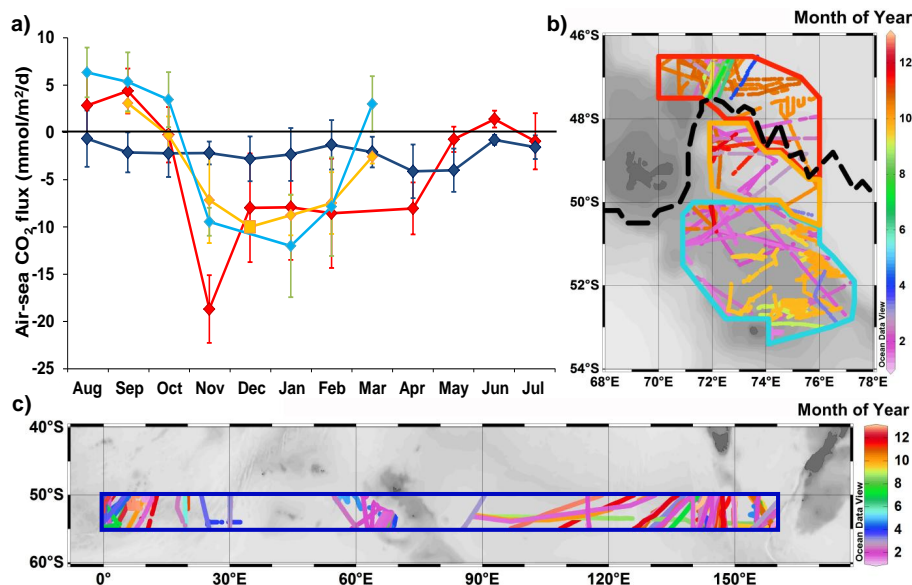


**Figure 7.** (a) Evolution of the mean air–sea CO<sub>2</sub> fluxes estimated in different regions of Kerguelen’s bloom (data shown in b): the Middle zone (orange), the Plateau south of 50° S (light blue) and the Polar Front zone (red), and compared to HNL waters found upstream and downstream of the Kerguelen Plateau (dark blue, data shown in c). The square symbol in panel a shows the mean value measured in December by the CARIOCA buoy launched during the KEOPS2 survey (L. Merlivat, personal communication, 2013). Diamonds show the monthly means obtained from the SOCAT-v2 database (1991–2008) completed with the recent OISO data (2010–2014, including the KEOPS2 survey).

Title Page

Abstract

Introduction

Conclusions

References

Tables

Figures

I◀

▶I

◀

▶

Back

Close

Full Screen / Esc

Printer-friendly Version

Interactive Discussion

